Available online at www.sciencedirect.com
ScienceDirect
Journal of Magnetic Resonance 186 (2007) 11–16
JMR Journal of Magnetic Resonance
www.elsevier.com/locate/jmr

A single-scan method for measuring flow along an arbitrary direction

H. Cho [a], X.-H. Ren [a], E.E. Sigmund [b], Y.-Q. Song [a,*]

[a] Schlumberger-Doll Research, One Hampshire Street, Cambridge, MA 02139, USA
[b] Department of Radiology, New York University, New York, NY 10016, USA

Received 23 October 2006; revised 3 January 2007
Available online 12 January 2007

Abstract

In this article, we demonstrate a single-scan method to measure an average flow velocity vector along an arbitrary direction. This method is based on the MMME sequence and utilizes static and pulsed magnetic field gradients along multiple directions for the optimal determination of flow velocity components in three-dimensional space. Experimentally measured average flow velocities from the flow induced phase shift with a single-scan MMME sequence show excellent agreements with the known flow rate, and the signal decay of each echo due to a velocity distribution is also quantitatively verified with known laminar flow patterns.

Keywords: MMME; Flow; Multiple echoes; Single-scan

1. Introduction

Flow velocities of various processes are often measured by NMR experiments with static or pulsed field gradients. The motion of spins induces a phase shift to the spatially modulated spin magnetization in the presence of a magnetic field gradient. This phase shift can be measured by conventional NMR methods such as gradient echo (GE), pulsed gradient spin echo (PGSE) or pulsed gradient stimulated echo (PGSTE) sequences [1–3]. There have been a growing number of applications where the phase encoding of a velocity is followed by fast imaging sequences to obtain a spatially resolved velocity map. EPI, FLASH and RARE imaging modules have been successfully applied to a velocity mapping to study various flow patterns [4–8]. Fast gas flow (>10 m/s) also has been measured with purely phase encoded MRI with flow sensitization [9].

On the other hand, for time-sensitive processes such as blood flow in medical applications or fluid characterization in well logging applications, it can be important to measure an average flow velocity vector as fast as possible without the need for a spatially resolved velocity map. The conventional NMR methods of a velocity encoding require independent scans for different gradient directions which may hamper the monitoring of time-dependent processes.

The multiple modulation multiple echo (MMME) sequence has recently been shown to be capable of measuring the magnitude of mean flow velocity along the applied gradient direction [10]. Here, we demonstrate that the MMME sequence can be extended to measure both the magnitude and the direction of the average flow in three-dimensional space in a single scan. Accordingly, this method does not require the alignment of a flow direction within the gradient coil geometry to obtain a flow velocity vector. This extension, motivated by a successful diffusion tensor measurement with the MMME sequence [11,12], is achieved by using a static gradient along one direction and pulsed field gradients along other directions.

2. Theory

In the presence of a magnetic field gradient ($\vec{g}$), the precession frequency of a spin-1/2 nucleus linearly depends on the position of spins. The spin magnetization becomes spatially modulated due to this dependence, and this

* Corresponding author. Fax: +1 617 768 2386.
E-mail address: ysong@slb.com (Y.-Q. Song).

1090-7807/$ - see front matter © 2007 Elsevier Inc. All rights reserved.
doi:10.1016/j.jmr.2007.01.004

modulation is often described by a time dependent $\vec{k}$ (spatial wave vector),

$$\vec{k}(T) = \gamma \int_0^T q(t)\vec{g}\mathrm{d}t, \tag{1}$$

where q is the coherence number of the magnetization state.

For molecules moving at a mean velocity $\vec{v}_{av}$ with a velocity distribution $P(\vec{v})$, the shift of the spatial modulation can induce a phase shift (ϕ_1) and the magnetization (M) can be written as,

$$M = M_0 e^{\mathrm{i}\vec{v}_{av}\cdot\vec{f}_Q} \int e^{\mathrm{i}(\vec{v}-\vec{v}_{av})\cdot\vec{f}_Q} P(\vec{v})\mathrm{d}\vec{v}, \tag{2}$$

$$\phi_1 = \vec{v}_{av}\cdot\vec{f}_Q \tag{3}$$

and

$$\vec{f}_Q = \gamma \int_0^T q(t)\vec{g}(t)t\mathrm{d}t. \tag{4}$$

The coefficient, $\vec{f}_Q$ denotes the sensitivity of the phase shift to the flow and M_0 refers to the magnetization in the case of no flow [10,13]. Q denotes the specific coherence pathway.

For the conventional flow sensitive gradient experiments (GE, PGSE, and PGSTE), only one $\vec{f}_Q$ value can be implemented in a scan so that at least three separate experiments with orthogonal gradient directions are needed to determine a flow velocity vector ($\vec{v}$) in three-dimensional space.

It has been shown that multiple echoes with different flow induced phase shift coefficients ($\vec{f}_Q$) can be produced with a few RF pulses in the presence of a constant field gradient [10]. The MMME sequence is also appealing for a fast flow velocity vector measurement because of the well-separated multiple echoes ($n = (3^{N-1} - 1)/2$, where n and N is the number of echoes and RF pulses, respectively). Detailed descriptions and various applications of the MMME sequence for diffusion measurements or imaging applications can be found elsewhere [14,11,15,12]. In this work, we concentrate on the flow induced phase shift.

In the case of flow with a distribution of velocity, Eq. (2) can be generally expanded to get,

$$M = M_0 e^{\mathrm{i}\vec{v}_{av}\cdot\vec{f}_Q}\left[1 + \mathrm{i}\int(\vec{v}-\vec{v}_{av})\cdot\vec{f}_Q P(\vec{v})d\vec{v} - \int\frac{((\vec{v}-\vec{v}_{av})\cdot\vec{f}_Q)^2}{2!}P(\vec{v})d\vec{v} + \cdots\right]. \tag{5}$$

When a distribution of velocity is symmetric about the mean velocity, the imaginary part in $[\cdots]$ in Eq. (5) vanishes, the flow induced phase shift (ϕ_1) is proportional to $\vec{f}_Q$, and the flow distribution causes a reduction in each echo's amplitude. An average flow velocity can be measured for a symmetric distribution of velocities. For non-symmetric velocity distributions [16,17], the imaginary part in $[\cdots]$ in Eq. (5) becomes non-zero and ϕ_1 is not exactly linear in $\vec{f}_Q$. Then the phase dependence on $\vec{f}_Q$ can be used to extract higher order moments of the velocity distribution [16].

3. Pulse sequence and optimization

Now, we describe the MMME sequence for measuring a flow velocity vector along an arbitrary direction. Consider a sequence given in Fig. 1. Thirteen well-separated echoes are formed following four RF pulses in the presence of a constant G_z gradient in a single scan. Each echo is the result of one specific coherence pathway. Appropriate pulsed field gradients along the x and the y directions are added to optimally determine flow velocity components in three-dimensional space, both in pulse sequence A (Seq. A) and pulse sequence B (Seq. B). Both sequences generate 13 distinct fully refocused ($\vec{k} = 0$) echoes. The gradient pulse sequence determines the 13×3 flow induced phase shift coefficient matrix of $F^{ij}(j = x,y,z, i = 1\text{–}13)$. We rewrite Eq. (3) in a matrix form to account for the flow induced phase shift of each echo in the MMME sequence in the presence of a flow velocity vector,

$$\Phi_1 = F \times V, \tag{6}$$

where $F^{ij} = [\gamma \int_0^T g_j t\ \mathrm{d}t]_i$, $V^j = v_j$ and $\Phi_1^i = \phi_1^i (j = x,y,z,$ $i =$ echo number).

An unique determination of V requires at least three linear equations or measurements. For over-determined systems (when there are more linear equations or measurements than unknowns), the least square solution that minimizes the residual error for V is given by [18],

$$V = (F^T \times F)^{-1} \times F^T \times \Phi_1. \tag{7}$$

The crosses indicate matrix multiplications. To obtain an optimized gradient sequence to get a reliable solution for V, we consider a well-known measure of the intrinsic error in linear equations. This value, referred to as the condition number [18,19], relates the relative error in the input data (Φ_1) to that in the output parameters (V),

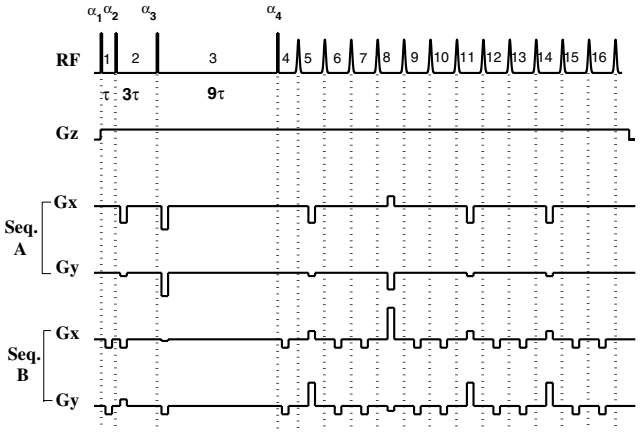

Fig. 1. The MMME pulse sequences optimized for a flow velocity measurement along an arbitrary direction. Seq. A has an advantage of less gradient switchings and Seq. B provides a lower condition number. Each number in the RF section labels the corresponding gradient pulse during each time interval.

$$\frac{\delta V}{V} = \mathrm{cond}(F)\frac{\delta \Phi_1}{\Phi_1}, \tag{8}$$

where $\mathrm{cond}(F) = \|F^{-1}\| \cdot \|F\|$ and $\|\cdot\|$ denotes norm. F^{-1} represents the pseudo-inverse when F is non-square matrix. Clearly, it is favorable to have a lower condition number if possible since it improves the accuracy of V with a given measurement error in Φ_1. On the other hand, we also want to reduce the number gradient switchings and prefer to use lower gradient values to minimize the effect of eddy currents. These are important issues, since the MMME sequence requires many refocusing gradient pulses to acquire the full train of echoes.

Seq. A has an advantage of less gradient switchings by having no pulsed gradient field during the period "1" in Fig. 1, and provides the condition number of 10. Omitting the pulsed field gradient during the period "1" is useful from a practical point of view because refocusing gradients are only needed before every three echoes. This feature was also utilized in the 2D diffusion measurement [11,12]. Seq. B can reach closer to the condition number of 1 but requires intensive gradient switchings before each echo. These sequences are representative for both pulsed gradient schemes with reasonable condition numbers but not necessarily the best gradient configuration for each case, because we limited the strength ($\leqslant$14 G/cm) and the duration (1 ms) of gradient pulses for both cases. We implement and compare the results of both sequences.

4. Materials and methods

The sample used in the experiment was a 5-mm NMR tube (inner diameter: 0.424 cm) connected to a continuous flow system (syringe pump 1000D, Teledyne ISCO, Inc., USA). Experiments were performed at a 2T horizontal bore magnet (Nalorac Cryogenics) operating at a proton frequency of 85.1 MHz. A Bruker Biospec spectrometer and a home-built 1 cm diameter saddle coil RF probe were used.

The 4-pulse MMME sequence in Fig. 1 was used with $\tau = 2$ ms. The combination of flip angles was [54°–71°–71°–110°], which are shown to provide the most uniform echo amplitudes and shapes among different echoes [14,15]. The $\pi/2$ pulse duration was 10 μs and the phases of RF pulses were all zero. The gradient values used for Seq. A and Seq. B in Fig. 1 are summarized in Table 1 and the duration of the gradient pulse along the x and the y direction was 1 ms. Seq. A and Seq. B have condition numbers of 10 and 4, respectively. Finally, a phase alternated 3 pulse MMME sequence with a constant gradient along the flow direction (z) was used to evaluate the magnitude of a fast flow velocity along the gradient direction.

As reference experiments, all sequences were initially executed for a stationary sample. The phase of receiver was adjusted until the imaginary signals were close to zero. Euler rotations of $R_z(\pi/4)R_y(\pi/4)R_z(\pi/4)$ and $R_z(0)R_y(0)R_z(\pi/4)$ were performed on the gradient sets' reference axes to implement 3D and 2D flow conditions within the existing gradient coil geometry, respectively. $R_\phi(\alpha)$ refers to a rotation about the ϕ axis by an angle α and any three dimensional rotation can be decomposed into the triplet of Euler angles as $R_z(\gamma)R_y(\beta)R_z(\alpha)$.

A phase change for each echo due to a flow (Φ_1, 13×1 matrix from Eq. (5)) was estimated by minimizing the imaginary part of each echo. A numerical phase, $\exp^{(-i\phi)}$ was applied to both the reference and the flow experiment until the integral of imaginary signal was zero, and the flow induced phase shift was obtained from $\phi_1 = \phi_{\min}^{\mathrm{flow}} - \phi_{\min}^{\mathrm{ref}}$. We note that with a adjusted receiver phase, the value of $\phi_{\min}^{\mathrm{ref}}$ for each echo is close to zero and no additional reference scan will be needed.

An amplitude reduction for each echo in the MMME sequence due to a velocity distribution can be calculated exactly with the known Pouiselle pipe flow distribution. $P(v)$ is $1/2v_{av}(0 < v < 2v_{av})$ for laminar flow. For this distribution, Eq. (2) becomes,

$$|M| = |M_0|\frac{\sin(v_{av}f_Q)}{v_{av}f_Q}. \tag{9}$$

This reduction in the signal amplitude for each echo is verified by comparing echo signal intensities for both the reference and the flow experiment for a 1D flow case.

Table 2 summarizes average flow velocities and the experimental parameters used in the experiments. An average flow velocity is obtained from dividing the volumetric flow rate by the cross sectional area of the NMR tube.

5. Experimental results and discussion

Fig. 2 compares the calculated phase shifts (derived from F and V values in Table 2) and the experimentally

Table 1
Gradient values used for the MMME sequences

Gradient pulse number	1	2	3	4	5	6	7	8	9	10	11	12	13	14	15	16
G_z for Seq. A,B	2	2	2	2	2	2	2	2	2	2	2	2	2	2	2	2
G_x for Seq. A	0	−10	−14	0	−10	0	0	6	0	0	−10	0	0	−10	0	0
G_y for Seq. A	0	−2	−14	0	−2	0	0	−10	0	0	−2	0	0	−2	0	0
G_x for Seq. B	−5	−5	−1	−5	5	−5	−5	19	−5	−5	5	−5	−5	5	−5	−5
G_y for Seq. B	−5	4	−5	−5	14	−5	−5	−3	−5	−5	14	−5	−5	14	−5	−5

Top row refers to the gradient pulse number as indicated in Fig. 1.
Seq. A and Seq. B have condition numbers of 10 and 4, respectively. The duration of each gradient pulse along the x and the y direction is set to 1 ms and the strength of gradient pulses are given in the unit of G/cm.

Table 2
Experimental sequence parameters used in various experiments

	Flow 1	Flow 2			
Experimental parameters	v_z, v_x, v_y (mm/s)	v_z, v_x, v_y (mm/s)	τ (ms)	δ (ms)	Number of RF pulses (N)
Seq. A, Seq. B with 1D	0.24, 0, 0	0.47, 0, 0	2	1	4
Seq. A, Seq. B with 2D	0.17, −0.17, 0	0.33, −0.33, 0	2	1	4
Seq. A, Seq. B with 3D	0.17, −0.12, 0.12	0.32, −0.24, 0.24	2	1	4
Fast flow with 1D	47.2, 0, 0	23.6, 0, 0	0.1		3

Seq. A and Seq. B refer to the different gradient sequence as shown in Fig. 1 and Table 1. 2D and 3D flow conditions are implemented by suitable rotations of the gradient sets' reference axes in the presence of uniform flow ((1) 0.24 mm/s, (2) 0.47 mm/s) along the z direction. τ and δ refer to the time spacing between echoes and gradient pulse length along the x and the y directions, respectively.

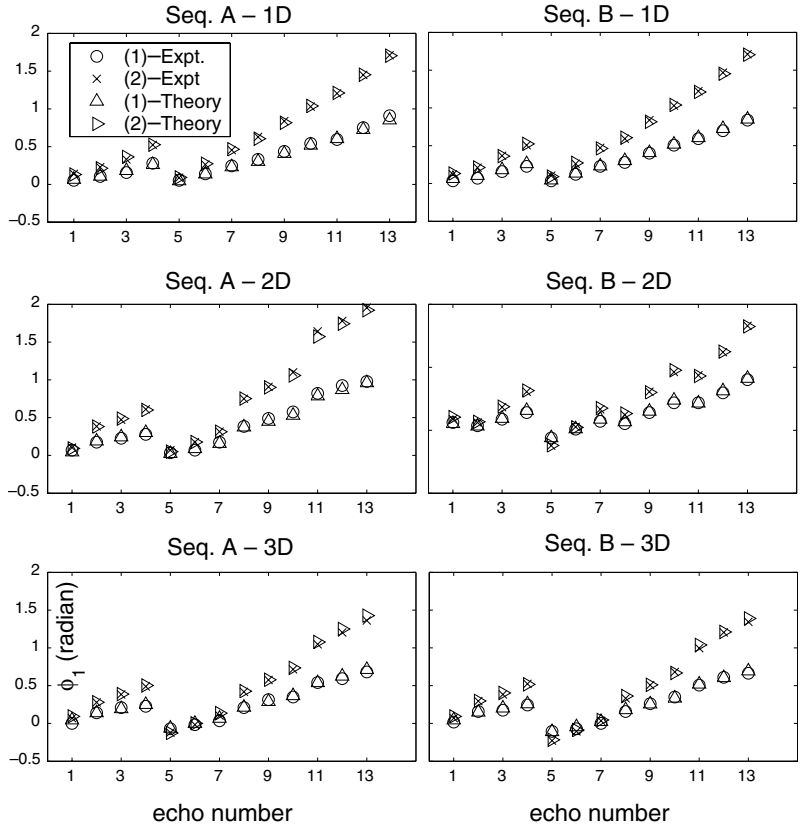

Fig. 2. Experimental results showing agreements between the calculated and the experimentally measured flow induced phase shifts. The sequence parameters of the corresponding experiments are listed in Table 2.

measured phase shifts for each echo from both Seq. A and Seq. B for various cases. Agreements between the theoretical and the experimental flow induced phase shift are excellent.

Fig. 3 verifies the echo signal decay due to a velocity distribution. Initially, a reference experiment with no flow condition was performed to obtain M_0 in Eq. (9) for each echo. In the top figure, expected signal reductions due to a velocity distribution are calculated from Eq. (9) and the calculated echo intensities are compared with the measured echo intensities from the flow experiments. In the bottom figure, each echo intensity (M) in the flow experiments is normalized to the corresponding echo intensity (M_0) from the reference experiment. This normalization cancels the effects of RF pulse flip angle, self-diffusion and relaxation from the echo amplitude data. The normalized echo intensities are shown with the theoretical calculations from Eq. (9). Their agreement quantitatively confirms the decay of echo signal from a velocity distribution.

Finally, Fig. 4 compares the flow velocity components in Table 2 and the corresponding least-square solutions for V from the measured flow induced phase shifts. Five separate experiments were performed for each condition for Seq. A and Seq. B to estimate the standard deviation of estimated V and are shown to fall within ~5% of mean velocities measured. Agreements between the actual velocity components and the measurements are outstanding. The velocities measured with Seq. A show a slightly larger standard deviation in the repeated measurements than those from Seq.

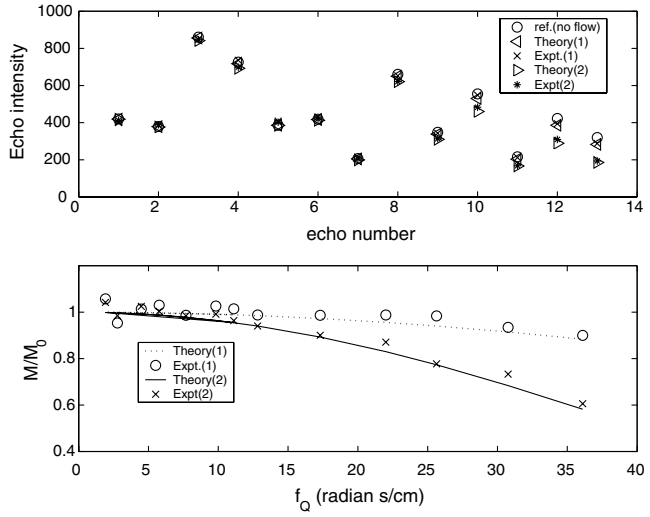

Fig. 3. Echo signal decay due to a velocity distribution. The top figure shows raw echo intensities for the reference experiment (no flow, ○) and experiments with two different flow velocities: (1) 0.24 mm/s(×); (2) 0.47 mm/s(∗). The calculated echo intensity from Eq. (9)(◁, ▷) is also plotted for comparison. In the bottom figure, each echo intensity in the flow experiments (M) is normalized to the corresponding echo from the reference experiment (M_0) and the normalized intensities are plotted with the theoretical calculations.

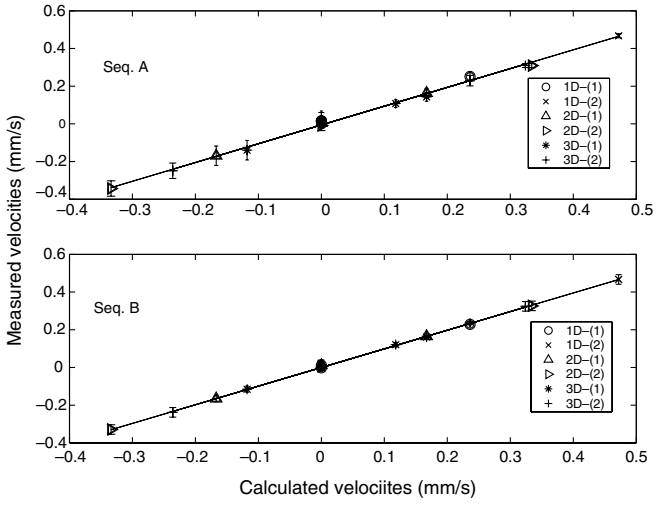

Fig. 4. Flow velocity components determined from the various experiments using least square solution from Eq. (6). A linear correlation between the calculated and the measured values are shown.

B, consistent with the sequences' different condition numbers.

The benefit and accuracy of a single-scan flow velocity vector measurement with the MMME sequence is clearly demonstrated in Fig. 4. On the other hand, it is worthwhile to consider the effective range of a flow velocity that can be measured from a specific MMME sequence with a given τ and gradient values.

For the 13-echo MMME sequence, the last echo acquires the maximum phase shift of $4.5g\nu\tau^2$ radians for a 1D flow. For a reasonable phase estimation without a phase overlap, we may set the limit for the available parameters for the sequence such that $4.5g\nu\tau^2 < \pi$. For example, the maximum flow velocity that can be measured by $g = 2$ G/cm and $\tau = 2$ ms is 0.09 cm/s. For the 4 echo, 3 pulse MMME sequence, the maximum phase shift on the 4th echo is 0.43 $g\nu\tau^2$ radians. For $g = 10$ G/cm and $\tau = 0.1$ ms, the maximum velocity that can be measured can be extended to 163 cm/s.

We also note that the flow induced phase shift depends linearly on g and quadratically on τ, which will make the shorter MMME sequences more attractive for a fast flow measurement. Furthermore, an RF phase alternation scheme demonstrated in Fig. 5 improves the separation of each echo by a factor of two, which enables a shorter MMME sequence with given gradient values. Fig. 5 shows the echo intensities for both channels for an experiment where the RF pulse phases were alternated between 0 and $\pi/2$ in successive pulses. The data quality demonstrates the benefit of the increased echo separation.

Fig. 6 shows the 1D flow velocity measurements for fast flow velocities using the phase alternation technique with $g = 10$ G/cm and $\tau = 0.1$ ms with the 3-pulse MMME sequence. The experimental results are in good agreement with the expected flow velocities which are showed in the legend of Fig. 6. The 3 pulse sequence, while not suitable for a 3D flow determination, provides a competitive scanning speed with the conventional single echo methods.

The extension of this work to more heterogeneous systems and/or to a spatially resolved flow measurement warrants some discussion. First, the stationary "reference" experiment may not be practical for in vivo flow imaging or ex-situ logging measurements. Fortunately, the phase measurement from which the flow is derived does not require this reference scan. However, the flow-based signal attenuation would be superposed on that from diffusion, so the velocity distribution sensitivity of the MMME sequence

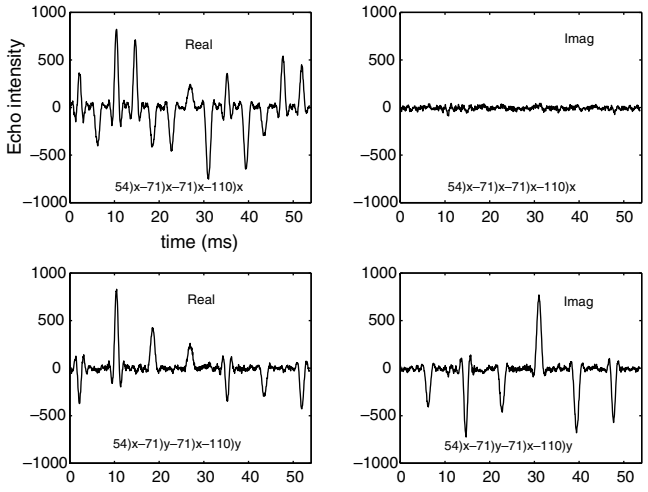

Fig. 5. Echo separation by a phase alternation scheme. Upper channels show the raw signals for the real and the imaginary part with same RF pulse phases and bottom channels with $\pi/2$ phase alternation in adjacent pulses.

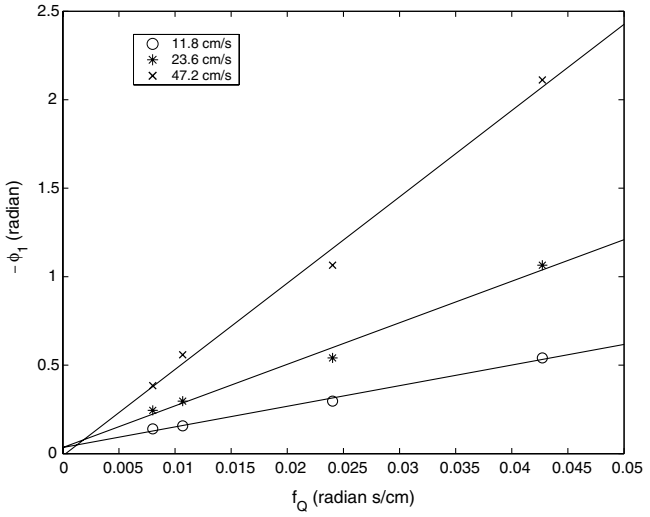

Fig. 6. The flow velocity estimated from each linear fit is 11.3 ± 0.9 cm/s, 24.3 ± 1.1 cm/s and 50.1 ± 2.7 cm/s for ○, ∗, and ×, respectively. The expected flow velocities are shown in the legend of Fig. 6 and the errors are estimated by the standard deviations of each measurement from the repeated experiments.

may be more difficult to exploit in practice. Also, although relaxation weighting does not affect the phase of the magnetization directly, sufficiently high relaxation rates in certain portions of the flow network may filter out those portions' phase contributions and skew the measured average flow. These effects will depend quantitatively on the system under investigation and should be considered in the use of MMME for flow applications.

6. Conclusion

We have shown that the MMME sequence can be extended for a measurement of an average flow velocity vector along an arbitrary direction in a single scan. The theoretical framework to understand the phase and the magnitude sensitivity of each echo of the MMME sequence was presented in the presence of a flow. We found an excellent agreement between the theory and the experiment for each of 1D, 2D, and 3D average flow velocity measurement, and quantitatively verified the origin of echo signal decay due to a velocity distribution for the case of a symmetric Pouiselle flow. For a non-symmetric flow, higher order moments of a velocity distribution can be inferred from the phase of each echo signal, and the MMME sequence with sufficiently many echoes may be used as a rapid method to obtain the information of a velocity distribution for a non-symmetric flow case.

In addition, the effective range of a flow velocity that can be measured from the specific MMME sequence is estimated. An echo separation technique from the RF phase alternation scheme is demonstrated and applied to a fast flow measurement with a short MMME sequence.

It was also shown that the normalization of each echo intensity to the corresponding echo intensity from the reference experiment without flow effectively eliminates the echo amplitude variations due to diffusion and relaxation effects.

This method will be applicable to mean flow velocity measurements for time-sensitive processes such as blood flow in medical MRI and fluid characterization in fast processes.

This work is supported in part by the National Institutes of Biomedical Imaging and Bioengineering (EB003869-01).

References

[1] E.L. Hahn, Spin echoes, Phys. Rev 80 (1950) 580.
[2] E.O. Stejskal, J. Tanner, Spin diffusion measurements: spin echoes in the presense of a time-dependent field gradient, J. Chem. Phys 42 (1965) 288.
[3] P.T. Callaghan, Principles of nuclear magnetic resonance microscopy, Oxford University Press, New York, 1993.
[4] K. Kose, Instantaneous flow-distribution measurements of the equilibrium turbulent region in a circular pipe using ultrafast NMR imaging, Phys. Rev. A. 44 (1991) 2495.
[5] S.-I. Han, P.T. Callaghan, One-shot velocimetry using echo planar imaging microscopy, J. Magn. Reson. 148 (2001) 349.
[6] A.J. Sederman, M.D. Mantle, C. Buckley, L.F. Gladden, MRI technique for meaurement of velocity vectors, accelaration, and autocorrelation functions in turbulent flows, J. Magn. Reson. 166 (2004) 182.
[7] M. Rokitta, U. Zimmermann, A. Haase, Fast NMR flow measurements in plants using FLASH imaging, J. Magn. Reson. 137 (1999) 29.
[8] B. Manz, Combined relaxation and displacement experiment: a fast method to acquire T2, diffusion and velocity maps, J. Magn. Reson. 169 (2004) 60.
[9] B. Newling, C.C. Poirier, Y. Zhi, J.A. Rioux, A.J. Coristine, D. Roach, B.J. Balcom, Velocity imaging of highly turbulent gas flow, Phys. Rev. Lett. 93 (2004) 154503.
[10] Y.-Q. Song, U.M. Schven, An NMR technique for rapid measurement of flow, J. Magn. Reson. 172 (2005) 31.
[11] X.-P. Tang, E.E. Sigmund, Y.-Q. Song, Simultaneous measurement of diffusion along multiple directions, J. Amer. Chem. Soc. 126 (2004) 16336.
[12] E.E. Sigmund, Y.-Q. Song, Multiple echo diffusion tensor acquisition technique, Magn. Reson. Imaging 24 (2006) 7.
[13] A. Sodickson, D.G. Cory, A generalized *k*-space formalism for treating the spatial aspects of a variety of NMR experiments, Prog. NMR Spectrosc. 33 (1998) 77.
[14] Y.-Q. Song, X.-P. Tang, A one-shot method for measurement of diffusion, J. Magn. Reson. 170 (2004) 136.
[15] H. Cho, L. Chavez, E. Sigmund, D.P. Madio, Y.-Q. Song, Fast imaging with the MMME sequence, J. Magn. Reson. 180 (2006) 18.
[16] U.M. Scheven, P.N. Sen, Spatial and temporal coarse graining for dispersion in randomly packed spheres, Phys. Rev. Lett. 89 (2002) 254501.
[17] R. Kubo, M. Toda, N. Hashitsume, Statistical physics II, Springer-Verlag, New York, 1991.
[18] G. Strang, Linear algebra and its applications, Brooks-Cole, Belmont, CA, 1988. (ISBN-10: 0155510053, ISBN-13: 978-0155510050).
[19] S. Skare, M. Hedehus, M.E. Moseley, T.-Q. Li, Condition number as a measure of noise performance of diffusion tensor data acquisition schemes with MRI, J. Magn. Reson. 147 (2000) 340.